Abstract

Prostate cancer, which causes over 30,000 deaths each year, is one of the most widespread cancers affecting the male population in the United States. Many genes have a role in the development of this disease, but the three main genes regulating cell division are *Pten*, *P53,* and *Phlpp2*. These genes have secondary impacts on metabolism because they affect the expression of *Akt* and *Myc*. The aim of this study was to gain further insight into the role of each gene in prostate cancer progression through the generation of organoids. As mouse-derived organoids have shown promise in modeling other forms of cancer, they were used for this study and analyzed with western blots and immunofluorescence. Immunofluorescence showed that organoid cells formed lobes resembling the shape of the prostate, but no luminal cells were found in the organoid. Additionally, Ki67 detection showed regions of high cell proliferation and tumor formation. Western blots also reinforced the relationship between cell division genes and metabolism genes. The results of this study reinforce the potential of mouse-derived in modeling prostate cancer. Organoid phenotypes matched with previously observed *in vivo* phenotypes for each genotype, and *in vivo* signaling pathways were maintained.

Introduction

A large disparity in survival rate exists between people diagnosed with metastatic prostate cancer (30%) and those diagnosed with non- metastatic prostate cancer (99%), but the cause of this disparity is unknown (ASCO, 2019). This may be due to effects non-tumor cells have on prostate cancer cells; it has been demonstrated that cultured cancer cells develop differently when exposed to normal body cells (Zhau et al, 1997). However, more research is necessary to reveal a connection between non-prostate cells and cancer cells. Organoids have the potential to save researchers time and money if they can model all of prostate cancer's phenotypes based on the set of mutations they express.

Organoids are a valuable tool in cancer research as they model internal conditions more accurately than traditional two dimensional cultures and allow for cell evolution. They can also transplanted into a mouse model to confirm results and link the *in vitro* results to *in vivo* results (Fumagalli et al, 2017; Lee et al, 2018). This allows researchers to assess the role of factors, such as metabolism and genomics, on cancer development or predict the effectiveness of a new drug (Walsh et al, 2016). Organoids have successfully been used to model multiple forms of cancer in the past. Breast cancer cells in human-based and xenograft-based organoids were able to model disease progression, drug response, and drug resistance (Walsh et al, 2014). Organoids are extremely useful for research, but they need to contain all of the cells located in the organ that is being recreated to be an effective model. Small changes in the type of cell present or concentration of various cells can have a large impact on organoid development (Campbell et al,

2011; Karthaus et al, 2014). However, human-derived prostate organoids are difficult to make, and the accuracy of mouse- derived prostate organoids in modeling aspects of prostate cancer is unknown (Risbridger, Toivanen, & Taylor, 2018).

Researchers have successfully used mouse models to gain tremendous insight into the metabolic and genetic aspects of cancer. This research has shown great variation within prostate cancer due to the activation of different genes and expression of different proteins. For example, AKT1 production mainly increases glycolysis and metabolism outside the mitochondria. Myc overexpression, on the other hand, leads to increased fatty acid metabolism and mitochondrial metabolism (Fan, Dickman & Zong, 2010; Priolo et al, 2010; Gouw et al, 2015). Various genes have been associated with these proteins and the development of prostate cancer. The *Phlpp2* gene is an important suppressor of AKT production, but it also stabilizes the Myc protein. *Phlpp2* inhibition in cancer cells has been shown to reduce cell division and metastasis (Nowak et al, 2019). These traits are enhanced when both the *Pten* and *P53* genes are deleted because this dual deletion increases *Phlpp2* expression (Nowak et al, 2015). Further, both *Pten* and *P53* are tumor suppressors, so their loss will facilitate formation of tumors (Ho et al, 2005; Kluth et al, 2014; Fumagalli et al, 2017). Deletion of the *Pten* gene alone, however, may not always cause the development of cancer (Radziszewska et al, 2008; Kim et al, 2009). This study looks to create and optimize a line of organoids to test the viability of organoids in modeling prostate cancer progression. It also looks to investigate prostate cancer genomics to determine the relationships between the genotypes of cancer cells and their phenotypes.

Materials and Methods

Generation and Culture of Organoids

Organoids were generated using prostate tissue from four distinct groups of mice: wildtype mice, *Pten*$^{loxP/loxP}$ mice (referred to as P), *Pten*$^{loxP/loxP}$ and *Trp53*$^{loxP/loxP}$ mice (referred to as 2P), and *Pten*$^{loxP/loxP}$, *Trp53*$^{loxP/loxP}$, and *Phlpp2*$^{loxP/LoxP}$ mice (referred to as 3P). Separate organoid lines were created for each genotype. Prostate tissue was minced and allowed to incubate for 90 minutes in a 20 mL suspension of TrypLe to break cells apart. The cell solution was then pelleted by centrifugation. The TrypLe supernatant was removed and cells were resuspended with a new 10 mL of TrypLe before being passed through a syringe and re-centrifuged. The TrypLe was removed again, but it was replaced with 2 mL of DMEM full medium instead of additional TrypLe. The suspension was passed through a cell filter to prevent large cell masses from being used in the organoid. Medium was removed by centrifugation. Cells were then resuspended in 88 uL of medium and 264 uL of matrigel (1:3 ratio), and they were plated to form eight organoid domes as shown in figure one. This process was individually carried out for each of the mouse genotypes. The organoids incubated upside down for one hour at 37℃ and 5% CO_2 to prevent sinkage into 2D. After incubation, 2 mL of DMEM full medium

was added and organoids were allowed to grow in the incubator. A six well plate was always used for culturing organoids.

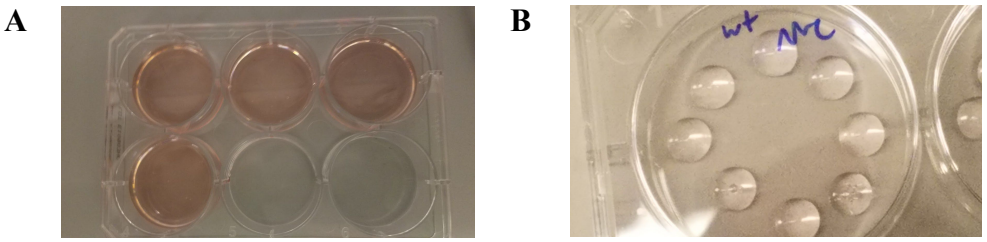

Figure One: Six well plate containing eight organoid domes with **(A)** and without **(B)** medium

Infection of Organoids

Organoids were infected with adenovirus containing Cre after three days of growth. Before infection occurred, organoids were detached from the plate using TrypLe, and they were washed using a wash buffer. The resulting suspension was moved into a centrifuge tube for a five minute incubation. Cells were then isolated from the solution by centrifugation and resuspended in 1.5 mL of DMEM full medium. The cell suspension was split into two groups, each containing 750 uL of the suspension. Adenovirus containing Cre was added into one of the suspensions; the other suspension became the no virus control (NVC) and received an equal amount of phosphate buffered saline (PBS). Cells incubated with the virus for three hours. The suspension was then centrifuged to pellet cells and allow the viral or PBS suspension to be aspirated. The cell pellet was resuspended in DMEM full medium (264 uL) and matrigel (792 uL). Each group of organoids (wild type NVC, wild type infected with Cre, etc.) was plated into three wells with six organoid domes in a well. Additionally, one organoid dome was plated on a slide well for immunofluorescence imaging. The infection process was repeated on multiple lines of organoids to determine the most effective method of infection. The first series of organoids was infected with adenovirus immediately after being resuspended in medium. 2.4 uL of the virus was added to each of the centrifuge tubes containing the experimental organoid groups. In response to the low infection success of this method, a second series of organoids was created. This series of organoids incubated in TrypLE for five extra minutes and was passed through a cell filter twice after being separated into the control and experimental tubes. These changes were made in an attempt to make the suspension consist of a higher percentage of single cells; this was predicted to allow greater infection efficiency.

Passaging of Organoids

One well of organoids from was passaged into three new wells to prevent over-confluence of cells as this can lead to sinkage or collapse into 2D. Passaging occurred three

days post-infection for all organoid groups. Organoids were detached from the well by a stream of TrypLE (200 uL to each dome). The TrypLE solution containing the organoids was gently mixed using a pipette before being moved to a falcon tube. Each group of organoids was added to a different falcon tube during passaging. Organoids shook at 200 rpm for five minutes in the TrypLE solution. Wash medium was then added (1 mL of wash medium for each dome) and the resulting solution was centrifuged (1,200 rpm) for three minutes to pellet cells. The supernatant was removed allowing the cell pellet to be resuspended in 264 uL of medium and 792 uL of matrigel. Organoids were then re-plated into three times the number of wells previously occupied.

Western Blot Analysis

A western blot was performed on two wells of organoids from each group to gain insight into infection success and expression of various onco-proteins. Cells in the organoid were lysed three days after organoids were passaged (three days and six days post-treatment) using 1×RIPA lysis buffer. Lysates were sonicated for ten cycles; each cycle consisted of 30 seconds of level high sonication followed by 30 seconds of rest. A 7 uL sample of the sonicated cell lysate was used for protein quantification, and a 63 uL sample was for electrophoresis. Concentrations were determined by the Eppendorf Plate Reader AF2200 based on the color the 7 uL lysate solution turned when combined with 686 uL of protein assay dye. Standards ranging from a concentration of 31.25 ug/mL to 2,000 ug/mL were created from BSA to calibrate the machine. The measured protein concentrations were used to load equal masses of proteins from the 63 uL sample into a gel. All gels for western blot analysis had a 7.5 mL resolving portion and a 3 mL stacking portion; both parts of the gel were 8% acrylamide. Gels were run for 2 hours at 100 volts before the results were transferred onto a membrane. The membrane sat in primary antibodies overnight and was exposed to secondary antibodies the next morning. The membrane was washed three times for ten minutes in a wash solution containing 1×TBS (Tris Buffered Saline) and 0.1% Tween before and after secondary antibody exposure. Hyperfilm was then exposed to the membrane for 15 second, 30 second, one minute, two minute, four minute, eight minute, and one hour intervals. Results were verified by applying □-actin antibody to all membranes and developing the results.

Immunofluorescence

Preparations for immunofluorescence (IF) imaging began the same day as western blot preparation started and organoid passaging occurred. To prepare organoids, the medium in the slide well was first replaced with 300 uL of 4% paraformaldehyde. Organoids were then washed in IF buffer (solution of 0.2% Triton X-10 and 0.05% tween in PBS) to remove the paraformaldehyde. Permeabilization solution was added to the wells to allow antibodies to enter the cell, and it was washed out with IF buffer after 30 minutes. Organoids then sat in blocking

solution containing primary antibodies overnight. Primary antibodies stained for CK5, CK8, Ki67, Pten, Myc, and Akt. Before secondary antibodies were added, the blocking solution was removed by washing organoids three times in IF buffer. DAPI was added at the same time as secondary antibodies. Both DAPI and the secondary antibodies were removed by washing the organoids in 300 uL of IF buffer for 15 minutes. IF buffer was then drained from the wells, and the chambers were detached leaving just the microscope slide with organoids. Each organoid dome was coated in 25 uL of ProLong Gold antifade mounting medium before sealing the slide with the cover slip. Imaging was conducted using the Zeiss 880 confocal microscope.

Results and Discussion

Organoid Structure

In order to ensure that organoids faithfully modeled prostate cancer, their structure and signaling pathways were analyzed. The androgen signaling pathway, an important signaling pathway in the prostate, was maintained in organoids that were infected with adenovirus containing Cre. IF imaging detected androgen receptor in the P organoid group as well as the 2P organoid group (Figure 2B). The hormone signaling pathway initiated by androgen receptor is prominent in the early development of prostate cancer (He et al, 2018), and as such, its presence in prostate cancer models is essential. In addition to detecting androgen receptor throughout the organoids, IF imaging also detected pockets of the cell proliferation indicator Ki67 in cancerous organoids (Figure 2C). Ki67 is an important indicator of tumor formation, so its detection in the mutated organoids advances their reliability in modeling prostate cancer. Combined, the presence of these two receptors and markers positively reflect on the ability of organoids to model prostate.

While organoids are accurate models of prostate cancer's biochemical aspects, they fail in fully resembling the appearance of a true prostate. Human and murine prostates contain two main types of epithelial cells that are involved in prostate cancer: basal cells which are marked by CK5 and luminal cells which are marked by CK8 (Choi et al, 2012). IF analysis of the organoids detected CK5 in all cells, but no CK8 was detected (Figure 2A and 2D). This shortcoming of organoids limits their reliability because interactions between luminal and basal cells will not occur. Since both cells are important in the inception of prostate cancer, and interactions between them are equally as important, organoids can not be complete models of the disease unless they contain basal cells and luminal cells. While these organoids do not have the same types of cells as the normal prostate, their shape resembles the prostate's shape; organoids formed circular lobes like those of the prostate (Figure 2A, B, D)

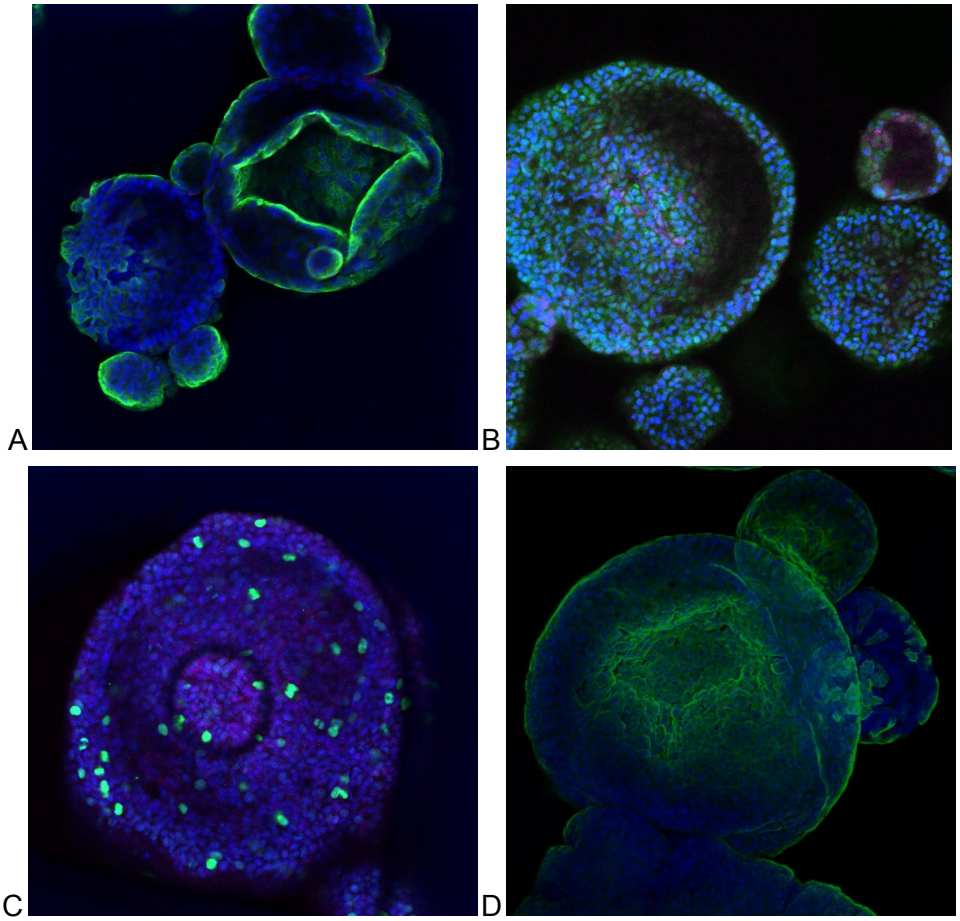

Figure 2: IF images of organoids (A) P organoids stained for CK5 (green), CK8 (magenta) and DNA (blue). **(B)** 2P organoids stained for androgen receptor (green), Pten (magenta) and DNA (blue). **(C)** 2P organoids stained for Ki67 (green), Pten (magenta) and DNA (blue). **(D)** Wild type organoids stained for CK5 (green), CK8 (magenta) and DNA (blue).

Knockout Success

Varying degrees of infection success and subsequent knockout of target genes were obtained between the two infection methods. *Pten* knockout had limited success in the first series of organoids (Figure 3A) as there was no decrease in Pten detection between the NVC organoids and mutated organoids after three days of growth. Western blots were conducted again after the organoids were passaged and had another three days of growth. However, the decrease in Pten detection was still minimal after six total days of growth (Figure 3B). This suggested that the infection success rate was low, and a deletion only occurred in some organoid cells after viral incubation. However, the second set of infection procedures yielded a greater infection success rate. Pten was only detected in the wildtype organoids, not in experimental organoids containing loxP sites, after one passage (Figure 3C). Furthermore, no Phlpp2 was

detected in 3P organoids (which contain loxP sites around the *Phlpp2* gene), but it was detected in all other organoids after day six (Figure 3D). This suggests that Cre virus can effectively knockout multiple genes at once and reduce associated protein expression in organoids. As such, organoids can be used to model specific prostate cancer genotypes for *in vitro* studies, and proper protein production can be verified by western blots.

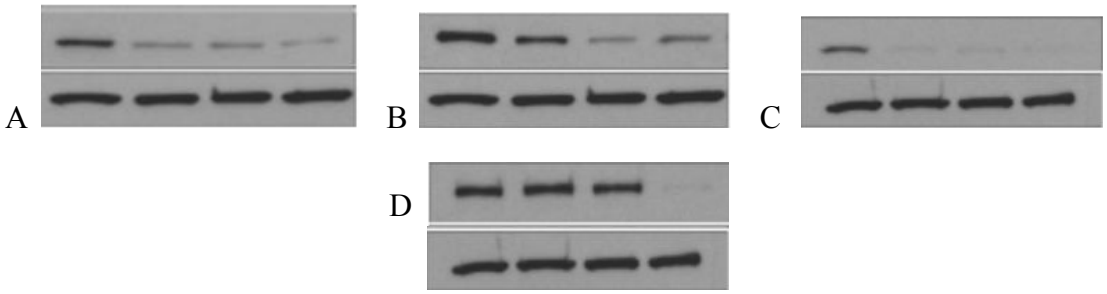

Figure 3: Western Blot Results (A) Pten detection (top) and B-actin (bottom) in day three organoids from the first series (left to right: wildtype, P, 2P, 3P) **(B)** Pten detection (top) and B-actin (bottom) in day six organoids from the first series (left to right: wildtype, P, 2P, 3P) **(C)** Pten detection (top) and B-actin (bottom) in day six organoids from the second series (left to right: wildtype, P, 2P, 3P) **(D)** Phlpp2 detection (top) and B-actin (bottom) in day six organoids from the second series (left to right: wildtype, P, 2P, 3P)

Downstream effects of knockouts

Western blots were also conducted to analyze the production of various other proteins associated with metabolism and growth. Wildtype and P organoids contained very little activated Akt protein as demonstrated by the lack of p-Akt1 detection for organoids in these groups. A high level of p-Akt1 was detected in the 2P organoids suggesting increased metabolic activity compared to wildtype and P organoids. p-Akt1 detection was elevated in 3P organoids, but it was less than in 2P organoids. Results for Myc concentration in the organoids followed the same trend; there was no Myc detected in P organoids, elevated Myc levels detected in 2P organoids, and a Myc level in between that detected in the P and 2P organoids in the 3P organoids. The overall pattern of these results reflects the increased metabolic activity of 2P organoids and the ability of a *Phlpp2* mutation that silences Phlpp2 production to reverse this increased metabolism (Fan, Dickman & Zong, 2010; Priolo et al, 2010; Gouw et al, 2015; Nowak et al, 2019). This suggests that inhibiting expression of the *Phlpp2* gene in patients with $Pten^{-/-}$ and $P53^{-/-}$ prostate cancer may reduce the malignancy of tumors and starve tumor cells of energy. Further research on the role of the Phlpp2 protein in prostate cancer development is necessary to explore this potential treatment option.

While Myc levels corresponded to previously established relationships between the genotypes tested in this study, Akt levels did not (Nowak et al., 2015). It was expected that Akt levels would be highest in the P organoids and lowest in the 2P organoids, but the opposite was

found. It is possible that *Pten* knockout alone was not sufficient to increase Akt expression and activation in the organoids. Organoids may need to be cultured with additional growth factors to increase similarity to a true prostate and ensure that results accurately reflect *in vivo* relationships. Although organoids can maintain macroscopic trends, these results indicate that they do not faithfully model all microscopic genomic relationships.

A  B 

Figure 4: Western Blot Results (A) p-Akt1 detection in day three organoids (left to right: wildtype, P, 2P, 3P) **(B)** Myc detection in day three organoids (left to right: wildtype, P, 2P, 3P)

Citations:

1. ASCO. (2019, June 06). Prostate Cancer - Statistics. Retrieved July 8, 2019, from https://www.cancer.net/cancer-types/prostate-cancer/statistics
2. Campbell JJ, Davidenko N, Caffarel MM, Cameron RE, Watson CJ (2011) A Multifunctional 3D Co-Culture System for Studies of Mammary Tissue Morphogenesis and Stem Cell Biology. PLoS ONE 6(9): e25661.https://doi.org/10.1371/journal.pone.0025661
3. N. Choi, B. Zhang, L. Zhang, M. Ittmann, L. Xin (2012) Adult murine prostate basal and luminal cells are self-sustained lineages that can both serve as targets for prostate cancer initiation. Cancer Cell, 21 (2012), pp. 253-265
4. Fan, Y., Dickman, K. G., & Zong, W. (2010). Akt and c-Myc differentially activate cellular metabolic programs and prime cells to bioenergetic inhibition. *Journal of Biological Chemistry,285*(10), 7324-7333. doi:10.1158/1535-7163.targ-09-b96
5. Fumagalli, A., Drost, J., Suijkerbuijk, S. J. E., Boxtel, R. van, Ligt, J. de, Offerhaus, G. J., ... Rheenen, J. van. (2017, March 21). Genetic dissection of colorectal cancer progression by orthotopic transplantation of engineered cancer organoids. Retrieved October 21, 2019, from https://www.pnas.org/content/114/12/E2357.
6. Gouw, A. M., Hsieh, A. L., Stine, Z. E., & Dang, C. V. (2015). MYC Regulation of Metabolism and Cancer. *Cancer Discovery,*1024-1039. doi:10.1007/978-3-7091-1824-5_5
7. He, Y., Hooker, E., Yu, E., Cunha, G. R., Liao, L., Xu, J., . . . Sun, Z. (2018). Androgen signaling is essential for development of prostate cancer initiated from prostatic basal cells. *Oncogene,38*(13), 2337-2350. doi:10.1038/s41388-018-0583-7
8. Ho, J. S., Ma, W., Mao, D. Y., & Benchimol, S. (2005). P53-Dependent Transcriptional Repression of c-myc Is Required for G1 Cell Cycle Arrest. *Molecular and Cellular Biology,25*(17), 7423-7431. doi:10.1128/mcb.25.17.7423-7431.2005

9. Karthaus, W., Iaquinta, P., Drost, J., Gracanin, A., Van Boxtel, R., Wongvipat, J., . . . Clevers, H. (2014). Identification of Multipotent Luminal Progenitor Cells in Human Prostate Organoid Cultures. Cell,159(1), 163-175. doi:10.1016/j.cell.2014.08.017
10. Kim, J., Eltoum, I. A., Roh, M., Wang, J., & Abdulkadir, S. A. (2009). Interactions between Cells with Distinct Mutations in c-MYC and Pten in Prostate Cancer. *PLoS Genetics,5*(7). doi:10.1371/journal.pgen.1000542
11. Kluth, M., Harasimowicz, S., Burkhardt, L., Grupp, K., Krohn, A., Prien, K., . . . Schlomm, T. (2014). Clinical significance of different types of p53 gene alteration in surgically treated prostate cancer. *International Journal of Cancer,135*(6), 1369-1380. doi:10.1002/ijc.28784
12. Lee, S. H., Hu, W., Matulay, J. T., Silva, M. V., Owczarek, T. B., Kim, K., . . . Shen, M. M. (2018). Tumor Evolution and Drug Response in Patient-Derived Organoid Models of Bladder Cancer. *Cell,173*(2), 515-527. doi:10.1016/j.cell.2018.03.017
13. Nowak, D. G., Cho, H., Herzka, T., Wang, V. M., Senturk, S., Demarco, D. V., . . . Trotman, L. C. (2015). Myc drives Pten/ p53-deficient proliferation and metastasis due to Il6-secretion and Akt-suppression via Phlpp2. *Cancer Discovery,*636-651. doi:10.1158/1538-7445.am2015-2258
14. Nowak, D., Dandrea, V., Watrud, K., Ambrico, A., Casanova-Salas, I., Buckholtz, C. L., & Trotman, L. C. (2019). The PHLPP2 phosphatase is a druggable driver of prostate cancer progression. *Journal of Cell Biology,218*(6), 1943-1957. doi:10.1158/1538-7445.am2018-109
15. Priolo, C., Pyne, S., Rose, J., Regan, E. R., Zadra, G., Photopoulos, C., . . . Loda, M. (2014). AKT1 and MYC Induce Distinctive Metabolic Fingerprints in Human Prostate Cancer. *Cancer Research,74*(24), 7198-7204. doi:10.1158/0008-5472.can-14-1490
16. Radziszewska, A., Choi, D., Nguyen, K. T., Schroer, S. A., Tajmir, P., Wang, L., . . . Woo, M. (2008). PTEN Deletion and Concomitant c-Myc Activation Do Not Lead to Tumor Formation in Pancreatic β Cells. *Journal of Biological Chemistry,284*(5), 2917-2922. doi:10.1074/jbc.m805183200
17. Risbridger, G. P., Toivanen, R., & Taylor, R. A. (2018). Preclinical Models of Prostate Cancer: Patient-Derived Xenografts, Organoids, and Other Explant Models. *Cold Spring Harbor Perspectives in Medicine,8*(8). doi:10.1101/cshperspect.a030536
18. Walsh, A. J., Castellanos, J. A., Nagathihalli, N. S., Merchant, N. B., & Skala, M. C. (2016). Optical Imaging of Drug-Induced Metabolism Changes in Murine and Human Pancreatic Cancer Organoids Reveals Heterogeneous Drug Response. *Pancreas,45*(6), 863-869. doi:10.1097/mpa.0000000000000543
19. Walsh, A. J., Cook, R. S., Sanders, M. E., Aurisicchio, L., Ciliberto, G., Arteaga, C. L., & Skala, M. C. (2014). Quantitative Optical Imaging of Primary Tumor Organoid Metabolism Predicts Drug Response in Breast Cancer. *Cancer Research,74*(18), 5184-5194. doi:10.1158/0008-5472.can-14-0663

20. Zhau, H. E., Goodwin, T. J., Chang, S., Baker, T. L., & Chung, L. W. (1997). Establishment of a three-dimensional human prostate organoid coculture under microgravity-simulated conditions: Evaluation of androgen-induced growth and psa expression. *In Vitro Cellular & Developmental Biology - Animal,33*(5), 375-380. doi:10.1007/s11626-997-0008-3